

## Time variations of the mean magnetic flux in active regions of different magneto-morphological classes

Anastasiya Zhukova<sup>1</sup>  ·  
 Valentina Abramenko<sup>1</sup> 

© The author(s) ••••

**Abstract** Using a recently suggested magneto-morphological classification (MMC, Abramenko, 2021, MNRAS Vol 507) of solar active regions (ARs), we explored 3048 ARs, observed from 12 May 1996 to 27 December 2021. Magnetograms were acquired with the Michelson Doppler Imager (MDI) on board the Solar and Heliospheric Observatory (SOHO) and with the Helioseismic and Magnetic Imager (HMI) on board the Solar Dynamics Observatory (SDO). ARs were separated between three classes: class A - regular ARs (bipoles which follow the empirical rules compatible with the mean field dynamo theory); class B - irregular ARs (“wrong” bipoles and multipolars); class U - unipolar sunspots. An aim of the present study is to explore time variations of a typical unsigned magnetic flux of ARs of different classes. The typical flux was acquired as the mean flux over all ARs of a given class observed during one solar rotation. The time profiles of the mean fluxes for different classes were compared. We found that, except for periods of deep solar minima, the mean flux of B-class ARs always dominate that of A-class ARs, and, what is the most important, the time profile of B-class ARs is highly intermittent versus the rather smooth and quasi-constant A-class profile. Intermittency implies a direct involvement of turbulence. We conclude that, through the entire active phase, the Sun is capable of producing regular moderate ARs at a quasi-constant rate along with the production of large and complex irregular ARs in the very intermittent manner. The result is the first observational evidence for the long-standing speculative assumption on the involvement of the convection zone turbulence into the regular global dynamo-process on a stage of the active regions formation.

**Keywords:** Active Regions, Magnetic fields; Magnetic fields, Photosphere; Turbulence; Instabilities

---

A.V. Zhukova  
[anastasiya.v.zhukova@gmail.com](mailto:anastasiya.v.zhukova@gmail.com)  
 V.I. Abramenko  
[vabramenko@gmail.com](mailto:vabramenko@gmail.com)

<sup>1</sup> Crimean Astrophysical Observatory of Russian Academy of Sciences, Nauchny 298409, Bakhchisaray, Republic of Crimea

## 1. Introduction

Active regions (ARs, groups of sunspots) on the surface of the Sun are widely known as the tracers of solar activity (see, e.g., a review by Hathaway 2015). They also are thought to bear the imprint of deep subphotospheric processes. Long-term observations of ARs have revealed a number of empirical patterns. In particular, the Spörer's law (Maunder 1903, 1904) describes the migration of sunspots in latitude during the 11-year Schwabe cycle. The Hale's polarity law (Hale et al. 1919) shows patterns of sunspot polarities during the 22-year cycle. These and other empirical rules gave an idea about the mutual transformation of the poloidal and toroidal components of the global magnetic field in the pioneer magnetic cycle models (Babcock 1961; Leighton 1964; Parker 1955) and formed the framework for the development of the mean-field dynamo theory (Moffatt 1978; Krause and Rädler 1980). However, even today, the diversity and variability of ARs generate new insights into the problems of magnetic field generation and dissipation.

It is well known that active regions come in different sizes. In the ARs area and magnetic flux distributions, two essential components were identified (Baumann and Solanki 2005; Zhang, Wang, and Liu 2010; Jiang et al. 2011; Muñoz-Jaramillo et al. 2015). The two corresponding populations of sunspot groups (small short-lived and large long-lived, Nagovitsyn et al. 2016) show differences in their essential properties (distribution by latitude, rotation speed, meridional velocities and other features, Nagovitsyn et al. (2018); Nagovitsyn, Ivanov, and Osipova (2019); Kutsenko (2021); Nagovitsyn, Pevtsov, and Osipova (2023); Gao and Xu (2024)). Large groups mainly provide the high level of the solar activity (Usoskin, Kovaltsov, and Chatzistergos 2016). The ratio of the numbers of small and large ARs varies on a secular time scale (Javaraiah 2013; Obrikko and Badalyan 2014). The Gnevyshev-Ohl rule (on the relative height of the even and odd cycles), the double-peak structure of a cycle manifest themselves in different ways for ARs of different sizes (Javaraiah 2012, 2016; Mandal and Banerjee 2016; Nagovitsyn and Osipova 2018).

Much attention is also paid to the magnetic configuration of active regions. Classification schemes are typically constructed based on the principle of increasing sunspot group complexity (Hale et al. 1919; McIntosh 1990; Abramenko 2021). The structural properties of individual sunspots and the ratio of large to small sunspots in a group are also in the focus of modern research (Knizhnik, Linton, and DeVore 2018; Mandal et al. 2021; Chowdhury et al. 2024; Nagovitsyn 2024). Observed bipolar active regions do not always exhibit a classical structure, for which both Hale's and Joy's laws (Hale et al. 1919) hold, and the dominant sunspot is located in the leading part of the AR (Grotrian and Künzel 1950; van Driel-Gesztelyi and Green 2015). Sometimes, an active region contains two close spots of opposite polarities within a common penumbra (a  $\delta$ -structure), which is often associated with high flare activity (Toriumi and Wang 2019).

The size and magnetic configuration of ARs are interrelated. Large ARs appear to be more complex (Kilcik et al. 2011). A scatter of the tilt angle (the angle between the equator and the axis connecting the leading and following parts of

the AR) depends on the AR's area (Wang and Sheeley 1989; Jiang, Cameron, and Schüssler 2014).

Depending on the phase of the cycle, the size and complexity of the ARs vary significantly. During the maximum phase, the largest groups appear (Mandal et al. 2017), and the proportion of complex groups increases to 30 percent (Jaeggli and Norton 2016). In contrast, during the minimum of the cycle, large groups do not appear, and the proportion of groups with complex magnetic configurations is less than one percent (Jaeggli and Norton 2016; Suleimanova and Abramenko 2024).

To reveal the role of complex ARs against the rest of ARs, the magnetomorphological classification (MMC) of ARs was recently proposed in the Crimean Astrophysical Observatory (CrAO) (Abramenko, Zhukova, and Kutsenko 2018; Abramenko 2021; Abramenko, Suleimanova, and Zhukova 2023). In accordance with the MMC, all sunspot groups are distributed between three classes: class A - regular ARs (bipoles which follow the empirical rules compatible with the mean field dynamo theory); class B - irregular ARs ("wrong" bipoles and multipolars); class U - unipolar sunspots (see Section 2 for details).

In our previous studies, we reported several interesting properties of irregular ARs: i) During the cycle maxima, the summed (over the disk) unsigned magnetic flux of all irregular ARs is about a half of that for all ARs, whereas their population consists only about a fourth of all (Abramenko, Zhukova, and Kutsenko 2018; Abramenko, Suleimanova, and Zhukova 2023); ii) The second peak of the maximum (in terms of the Gnevyshev's double-peak structure of a solar maximum, Gnevyshev 1963) in the solar cycle 23 (SC 23) and the solar cycle 24 (SC 24) seems to be produced by irregular ARs (Abramenko, Suleimanova, and Zhukova 2023); iii) Irregular ARs are found as the main producers of strongest X-class flares, especially during the second peak and the declining phase of a cycle (Abramenko 2021); iv) Irregular ARs seem to be responsible for a noticeable north-south asymmetry of the sunspots formation (Zhukova et al. 2023; Zhukova 2024; Zhukova, Abramenko, and Suleimanova 2024).

The above results of comparing regular and irregular ARs allowed us to make a qualitative conclusion in our previous studies that the generation of regular ARs is driven by the global dynamo, whereas the complexity of the magnetic structure of irregular ARs can be explained by the influence of the turbulent component of the dynamo inside the convection zone (Kitchatinov 2014; Sokoloff, Khlystova, and Abramenko 2015). If this is true, then the behavior of regular and irregular ARs should exhibit certain quantitative differences inherent to the enhanced turbulence (for example, highly intermittent time profiles of various parameters, or fast growth of high statistical moments, or heavy-tailed distribution functions, etc, see, Frisch (1995)). These considerations motivated us to seek for an approach that would allow us to demonstrate a quasi-smooth temporal development of regular ARs against the highly intermittent development of the irregular ARs. In case of affirmative answer, this result will be the first observational evidence for the involvement of the convection zone turbulence into the regular global dynamo-process on a stage of the active regions formation.

We focus on an analysis of irregularities in time variations of a typical unsigned magnetic flux of an active region for ARs of different classes. The typical flux

was acquired as the mean flux over all ARs of a given class observed during one solar rotation. The time profiles of the mean fluxes for different classes were compared.

## 2. Data and method

Unsigned magnetic flux data for ARs were acquired from magnetograms recorded from 12 May 1996 to 27 December 2021. For SC 23, full-disk line-of-sight (LOS) magnetograms were recorded with the Michelson Doppler Imager (MDI) instrument on board the Solar and Heliospheric Observatory (SOHO, Scherrer et al. 1995). The SC 24 data (starting on 16 June 2010) were acquired with the Helioseismic and Magnetic Imager (HMI) instrument on board the Solar Dynamics Observatory (SDO, Scherrer et al. 2012). LOS magnetograms from the Space-weather HMI Active Region Patches (SHARP, `sharp_cea_720s`) were used (Bobra et al. 2014). Details of the unsigned magnetic flux calculations can be found in Abramenko, Suleymanova, and Zhukova (2023).

Information on the distribution of ARs by MMC-class was acquired using the earlier compiled catalog of ARs where the MMC-class and unsigned magnetic flux are presented for each AR. The first version of the catalog was compiled in 2017 for SC 24 only (Abramenko, Zhukova, and Kutsenko 2018; Zhukova 2018). In 2022 the catalog for the SC 24 was updated by A. Zhukova in accordance with a new concept of classification (Abramenko 2021) and extended by R. Suleymanova to SC 23 (Abramenko, Suleymanova, and Zhukova 2023). The catalog contains data for 3048 ARs that appeared on the disk every 9th day from 12 May 1996 to 27 December 2021. The catalog is available at <https://sun.crao.ru/databases/catalog-mmars>.

The original aim for compiling the catalog was to separate the flux summed from all ARs presented on the disc at a given moment into several categories according to MMC-classes. For this purpose, we needed independent snapshots of the Sun continuously covering the solar surface without overlapping. The Sun makes a full rotation during approximately 27 days. Taking a full-disc magnetogram each 9th day and limiting the area of interest to a 60° distance from the central meridian, we cover approximately 120° along the longitude. Making three steps, we cover the entire solar surface without overlapping. Each AR was counted only once. In very rare cases, when the flux-weighted center of gravity of an AR was located closer than 60° at the both eastern and western limbs, we also counted the AR only once.

A shortcoming of this routine would be a possible omitting of ARs that lived less than 8 days. According to Nagovitsyn, Pevtsov, and Osipova (2017, figures 3, 4), the short-lived ARs have predominantly a small area, less than approximately 50 MSH (millionth of solar hemisphere). According to Muñoz-Jaramillo et al. (2015, figure 6), such small ARs have a total flux of less than  $10^{21}$  Mx. Note, that compiling the catalog, we counted ARs with the unsigned flux of above  $10^{21}$  Mx (Abramenko, Suleymanova, and Zhukova 2023). So, the possibly omitted ARs were anyway below our detection limit.

### Magneto-morphological classification of ARs (CrAO)

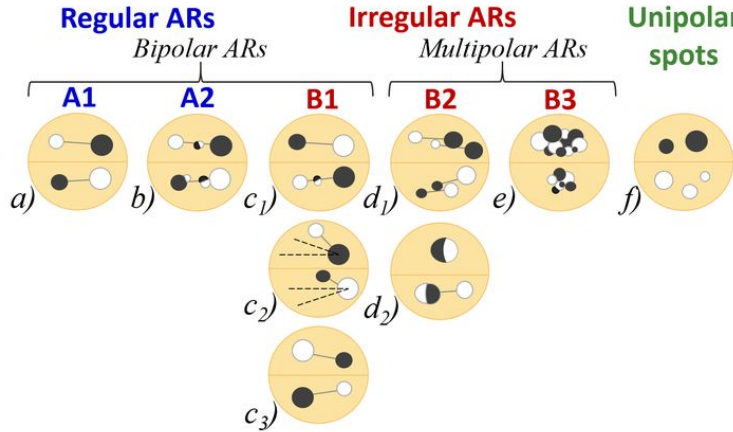


**Figure 1.** A sketch of the magneto-morphological classification. Sketch  $c_1$  represents violation of Hale polarity law,  $c_2$  - violation of Joy's law,  $c_3$  - violation of a rule of the leading spot's dominance. Sketches  $d_1$  and  $d_2$  represent various schemes of a distortion and fragmentation of a single flux tube. Sketch  $e$  represents a simultaneous appearance of several intertwined flux tubes. Sunspot polarities are shown for even cycles.

A sketch to illustrate the classification procedure for an even cycle is presented in Figure 1. Regular A-class bipolar structures (see Figure 1a) are oriented approximately along the east-west direction and obey Hale's polarity law (Hale et al. 1919) with the negative polarity leading spots in the N-hemisphere, they are consistent with Joy's law (Hale et al. 1919). Besides, the leading spot has to be larger, more compact than the following one (Grotrian and Künzel 1950; van Driel-Gesztelyi and Green 2015). So, these ARs in the best possible way follow the empirical laws (van Driel-Gesztelyi and Green 2015) compatible with the classical magnetic cycle models (Babcock 1961; Leighton 1964; Parker 1955). This allows us to presume that they are associated with the toroidal field produced by the global dynamo with minimal influence of the convection zone turbulence (Abramenko 2021; Abramenko, Suleymanova, and Zhukova 2023). Note, however, that the A2-class allows small  $\delta$ -structures inside (see Figure 1, b) and thus, a small influence of turbulence. Unipolar spots are gathered in a separate class U (see Figure 1f). All the rest form an ensemble of irregular ARs and belong to the class B (see Figure 1c, d, e).

Let us briefly explain the sampling routine illustrated in Figure 1. The statistical results are presented in Table 1.

Identification of A-class ARs is described above. Let's continue with class B1 (see lines 4-6 in Table 1 and marks  $c_1-c_3$  in Figure 1). The most difficult task was to identify "violators" of Hale polarity law (so called, anti-Hale ARs, or ARs of reverse polarity, see Figure 1,  $c_1$ ). In addition to identifying the reverse polarity, one more problem arises. During the overlapping of two consecutive cycles, high-latitude ARs of new cycle could be mistakenly counted as anti-Hale ARs of old cycle. To avoid this obstacle, the distribution of ARs between cycles was carried

out according to the technique suggested by McClintonck, Norton, and Li (2014). The high-latitude ARs located (on the time-latitude diagram) to the right from a cycle boundary, were considered as regular ARs of a new cycle. The subset of reverse polarity ARs is marked as HN (from Hale No) in Table 1. They consist only 1.7% from the total number of ARs. More details can be found in Zhukova et al. (2020, see Subsection 2.2. Ambiguities in anti-Hale region identification, point *i*) and Zhukova et al. (2022, see Subsection 3.1 Determination of a hosting cycle for each AR).

To identify "violators" of Joy's law of bipolar structures (see Figure 1, *c2*), we, following to Wang and Sheeley (1989), explored the orientation of the axis connecting the leading and following parts of an AR. Joy's law was counted to be met in cases when the axis was located between the two dashed segments forming an angle of 20° with the equator's direction. Two typical situations of "violation" of Joy's law are shown in the N- and S-hemispheres in Figure 1, *c2*. This subset is marked as JN (from Joy No) in Table 1.

It was rather straightforward to identify bipolar ARs, where the largest spot of the following polarity would be a dominant feature in the AR (see Figure 1, *c3*). This subset is marked as LN (from Leader No) in Table 1.

Compliance or violation of each aforementioned rule was marked with a flag: Y (for YES), or N (for NO) in the corresponding column in the MMC-catalog. Some "wrong" dipoles violated more than one rule and, so, they have more than one N-flag. They are also classified as B1-class ARs. That is why the summed quantity of HN+JN+LN exceeds the number (578) of B1-class ARs. The B1-class ARs can be considered as a result of mild distortion of a single toroidal flux tube owing to the convection zone turbulence.

Magnetic structures with a single dominant spot and no pores in the following part were identified as a class of unipolar spots, U, with two subclasses: U1 (without small magnetic elements of opposite polarity in the vicinity) and U2 (with numerous small magnetic elements of mixed polarity around).

The B2-class ARs were considered as offprints of strong turbulent distortion of a single flux tube. They are multipolar ARs consisting of two (or more) coaligned dipoles with the general orientation in accordance with Joy's law. A typical representative is NOAA AR 11158. Such ARs can be regarded as the result of fragmentation and distortion of a toroidal flux tube. ARs with a dominant  $\delta$ -structure (similar to NOAA AR 10930), considered as a kinked tube (see, e.g., Toriumi and Wang 2019, Sec. 4.1.1), also were classified as B2-class ARs.

The B3-class represents the most complex magnetic structures which can be considered as a result of interaction (intertwining) of several flux tubes in the convective zone. These ARs consist of opposite polarity spots distributed chaotically so that it is impossible to define the AR axis and assign leading and trailing sunspots. It is assumed that these ARs suffered the most from subphotospheric turbulence.

An increase of the influence of the convection zone turbulence is obvious when proceeding from A1- to B3-class. Thus, the MMC allows us to reveal and to order the influence of subphotospheric turbulence on the ARs appearance.

The list of B2 and B3 ARs (including their NOAA identifier and MMC class) is provided as Supplementary materials. A fragment is given in Table 2.

**Table 1.** ARs statistics for different MMC classes.

Class	A1	A2	B1	B2	B3	U1	U2	Total
Number	1402	104	578	203	180	403	178	3048
Ratio, %	46.0	3.4	19.0	6.7	5.9	13.2	5.8	100
Class								
			HN	JN	LN			
Number			52	336	300			
Ratio, % <sup>1</sup>			1.7	11.0	9.8			

<sup>1</sup>From total number

**Table 2.** Multipolar ARs of B2 and B3 classes.

NOAA	Date D/M/Y	Latitude	Longitude	Flux, Mx	MMC class
7962	12 05 1996	-6.68	-16.81	2.269E+022	B2
7978	05 07 1996	-8.97	-32.31	4.749E+021	B3
7981	01 08 1996	-10.07	-21.09	2.794E+022	B3
...					
12916	27 12 2021	-16.53	-14.90	2.660E+022	B2

From the catalog, we have the MMC-class and the unsigned magnetic flux for each AR. This allows us to calculate the number of ARs of a given class per one rotation, as well as the summed unsigned flux from them. Dividing the latter over the former, we obtain the mean flux for a given rotation for a given class. We also acquired time profiles for joined classes, say, A1+A2, by the same way: all ARs of A1 and A2 classes were used to get their total number and flux. A traditional 13-rotation moving average produces a time profile of the mean flux for a given MMC-class (see Figures 2, 3). A similar averaging method was used by Javaraiah (2013); Nagovitsyn, Osipova, and Nagovitsyna (2021) for long-term series of observations (about 140 years) with averaging over the annual time intervals.

Data on the total area of sunspots from the United States Air Force/National Oceanic and Atmospheric Administration Solar Region Summary (USAF/NOAA SRS) at <http://solarcyclescience.com/activeregions.html> were used to illustrate the general course of the cycles, (Figures 2, 3, top frames). The data were smoothed using the same method, averaging over 13 rotations.

### 3. Temporal variations of the mean flux in regular and irregular ARs

This section compares the mean magnetic flux data for A-class and B-class ARs. The results are shown in Figure 2. In the middle frame, the blue curve shows the result for the ensemble of all regular ARs (class A), while the red curve

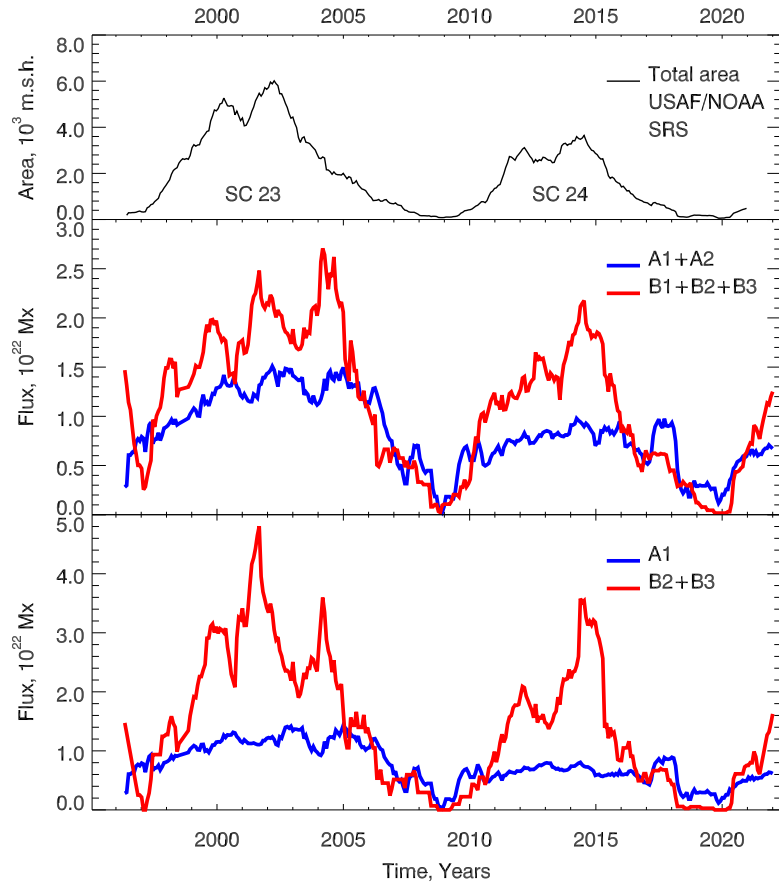


**Figure 2.** Time variations of the mean magnetic flux for A-class (blue) and B-class (red) ARs. For convenience, the total area of sunspots (in MSH) by USAF NOAA SRS illustrates the cycle progress (top frame).

shows the result for the ensemble of all irregular ARs (class B). In the bottom frame, the curves for the simplest A1-class dipoles and for the most complex ARs (multipolar of B2- and B3-classes) are presented.

During most of the active phase (an interval from the mid-rising phase to the mid-declining phase), the fluxes of A-class ARs are one and a half to two times (up to four times, for the data in the bottom frame) lower than the fluxes of B-class ARs. This means that the irregular ARs, on average, are considerably larger than the regular ones. What is the most interesting is the highly intermittent jagged profile for the B-class against a rather smooth and quasi-constant A-class profile. This tendency becomes more obvious when we move on to comparing extreme situations, setting side by side the simplest dipoles and the most complex multipolars, see Figure 2, bottom frame. This figure allows us to conclude that the Sun is capable to produce regular A1-class ARs approximately of the same

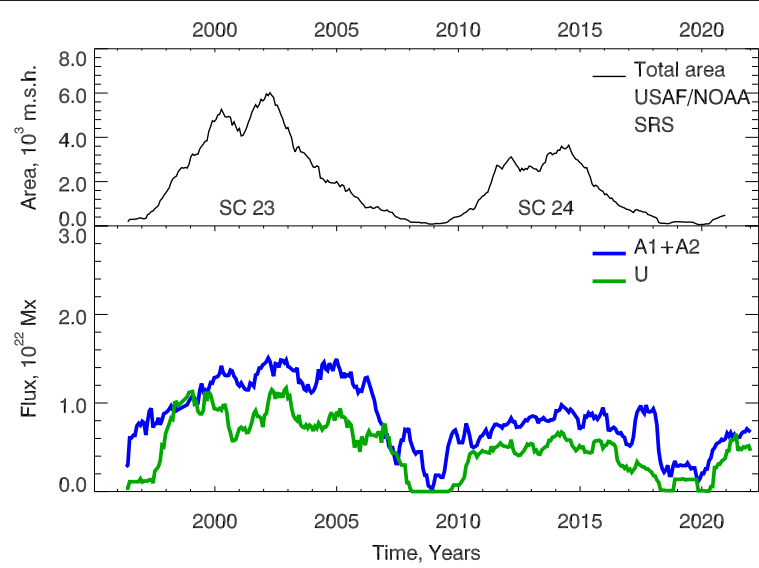


**Figure 3.** Time variations of the mean magnetic flux for A-class (blue) and U-class (unipolar sunspots, green) ARs. Notations are the same as in Figure 2.

flux of about  $(1 - 1.5) \times 10^{22}$  Mx constantly through the entire active phase, along with the production of complex multipolars of a broad range of fluxes (from 1 to  $5 \times 10^{22}$  Mx) in the very intermittent manner.

Besides, the middle frame in Figure 2 shows that, in the both cycles, the mean flux of B-class ARs shows a tendency to increase as the rising and maximum phases of a cycle proceed, and reaches a peak value at the beginning of the declining phase. It is consistent with the well-known observational fact that the large ARs with intricate magnetic configuration frequently occur during the declining phase. Such ARs are usually responsible for extreme flares (Abramenko 2021).

#### 4. Temporal variations of the mean flux in regular ARs and unipolar spots

Figure 3 represents the mutual variations of the mean fluxes of the A-class and U-class ARs. The amplitude correlates with the cycle strength (for the weak SC 24, both profiles are lower than that for the strong SC 23). Similar to the A-class profile, the U-class profile shows slightly flattened shape during the rising, maximum and the beginning of the descending phases, as if the shape of a solar maximum observed in the sunspot area (see top frames in Figure 3) was smoothed and lowered here. The level of the mean flux of U-class ARs in SC 23 is about  $0.8 \pm 0.2 \cdot 10^{22}$  Mx and  $0.5 \pm 0.1 \cdot 10^{22}$  Mx in SC24. Note that in Abramenko, Suleymanova, and Zhukova (2023, Figure 4a) we reported that the level of the summed flux for U-class ARs is approximately the same in both cycles. The lowered mean flux along with the same summed flux implies that

the unipolar sunspots were more numerous (or long-lived) in SC24 as compared to SC23.

The similarity of the time profiles of A-class and U-class ARs allows us to conclude that the origin of these types of ARs is the same, the regular global dynamo action with negligible influence of the turbulent component of dynamo. The common origin of A-class and U-class profiles is also supported by a well-known observational fact that a majority of unipolar spots are the remnants of the more compact and large leading spots of bipolar active regions.

## 5. Concluding remarks

Exploring the temporal behavior of the typical (in other words, mean) magnetic flux for active regions of different magneto-morphological classes, namely, simple dipoles (A-class), “wrong” dipoles and complex multipolars (B-class), unipolar sunspots (U-class), for two solar cycles (SC 23 and SC 24), we found the following.

Through the entire active phase (from the mid-rising to the mid-declining phase),

- the mean magnetic flux of the B-class (irregular) ARs significantly exceeds (up to 4 times) that of the A-class (regular) ARs;
- the mean magnetic flux of A-class ARs undulates in a quasi-uniform manner around the level of  $1.3 \cdot 10^{22}$  Mx in SC23 and  $0.8 \cdot 10^{22}$  Mx in SC24. At the same time, the B-class ARs demonstrate a highly **intermittent** profile with a broad range of mean fluxes, from 1 to  $5 \times 10^{22}$  Mx.
- the intensity of peaks in the B-class profile tends to be enhanced as the active phase proceeds.

Therefore, we conclude that the Sun is capable of producing regular moderate ARs at a quasi-constant rate through the entire active phase, along with the production of large and complex irregular ARs in the very intermittent manner. Any intermittent irregularities are an attribute of an influence of turbulence. So, we found the first observational evidence for the simultaneous action of the traditional regular mean-field dynamo and the turbulent component of dynamo on a stage of the active regions formation.

This finding allows us to explain one interesting observational phenomenon: strong, complex ARs tend to appear at the descending phase. As a cycle proceeds toward the descending phase, the convection zone becomes more contaminated by magnetic remains which interact with the coherent toroidal field lines and, with the assistance of turbulence, eventually initiate an enhanced production of complex irregular ARs on the surface. This is a reason why the most strong and complex ARs tend to occur closer to the end of the maximum phase and to the beginning of the descending phase.

The suggested above scenario of the mutual action of the traditional global dynamo and the turbulent component of dynamo will help shed light on the irregularities in the flux reversal process. Indeed, the decay of irregular ARs contaminates the quasi-regular pattern of meridional flows, formed by the drift to poles of debris of fragmented following parts of regular ARs. This, in turn,

leads to fluctuations and disruptions in the flux reversal process and influences the oncoming cycle performance, as it follows from observations (Mordvinov and Kitchatinov 2019; Mordvinov et al. 2022). Numerical simulations by Nagy et al. (2017) demonstrate that peculiarities are reinforced after the flux reversal (in other words, as the descending phase approaches). Moreover, authors argue: “... even a single “rogue” bipolar magnetic region (BMR) in the simulations can have a major effect on the further development of solar activity cycles, boosting or suppressing the amplitude of subsequent cycles.”

Apparently, the MMC-approach has a serious physical background, allowing us to visualize offprints of the turbulent component of dynamo.

We have shown here that it is the B-class ARs that turn out to be the most powerful in sense of magnetic budget. In this regard, the relationship of such ARs with strong flares, solar energetic particles and Ground Level Enhancements (GLEs) events (Abramenko 2021; Kashapova et al. 2021; Suleymanova, Miroshnichenko, and Abramenko 2024) becomes more clear. Strong flares and geoeffective events are widely associated with the large complex multipolar ARs and ARs with  $\delta$ -structures (see, e.g., Chen et al. 2011; Guo, Lin, and Deng 2014; Gao 2019; Norton et al. 2022; Kutsenko, Abramenko, and Plotnikov 2024).

We also revealed some interesting properties of unipolar sunspots. First, basing on a similarity in time profiles of the mean flux of A-class and U-class ARs, we presume that the origin of both types of ARs is the same, namely, the regular global dynamo action. Second, the weaker a cycle, the lower is the typical magnetic flux of unipolar sunspots. Besides, in the weak cycle (as compared to the strong cycle), the total number of unipolars could be higher, or they could survive longer (for several solar rotations). The result deserves further attention because an evolution of unipolar sunspots is closely related to the problems of the magnetic flux removal from the solar surface.

**Acknowledgements** Authors thank the anonymous referees for suggestions that improved the quality of this manuscript. SOHO is a cooperative international project between ESA and NASA. SDO is a mission for NASA Living With a Star (LWS) program. The SOHO/MDI and SDO/HMI data were provided by the Joint Science Operation Center (JSOC). The study was supported by Russian Science Foundation grant 25-12-00026.

**Author Contribution** AZh proposed a method for acquisition of mean fluxes, performed calculations, figures preparation. VA provided the task formulation and conclusions. Both authors worked on the text writing.

**Funding** Russian Science Foundation, grant 25-12-00026.

**Data Availability** No datasets were generated or analysed during the current study.

## Declarations

**Conflict of interest** The authors declare no conflict of interests.

## References

Abramenko, V.I.: 2021, Signature of the turbulent component of the solar dynamo on active region scales and its association with flaring activity. *Mon. Not. R. Astron. Soc.* **507**, 3698. DOI. [ADS](#).

Abramenko, V.I., Suleymanova, R.A., Zhukova, A.V.: 2023, Magnetic fluxes of solar active regions of different magneto-morphological classes - I. Cyclic variations. *Mon. Not. R. Astron. Soc.* **518**, 4746. [DOI](#). [ADS](#).

Abramenko, V.I., Zhukova, A.V., Kutsenko, A.S.: 2018, Contributions from Different-Type Active Regions Into the Total Solar Unsigned Magnetic Flux. *Geomag. Aeron.* **58**, 1159. [DOI](#). [ADS](#).

Babcock, H.W.: 1961, The Topology of the Sun's Magnetic Field and the 22-YEAR Cycle. *Astrophys. J.* **133**, 572. [DOI](#). [ADS](#).

Baumann, I., Solanki, S.K.: 2005, On the size distribution of sunspot groups in the Greenwich sunspot record 1874-1976. *Astron. Astrophys.* **443**, 1061. [DOI](#). [ADS](#).

Bobra, M.G., Sun, X., Hoeksema, J.T., Turmon, M., Liu, Y., Hayashi, K., Barnes, G., Leka, K.D.: 2014, The Helioseismic and Magnetic Imager (HMI) Vector Magnetic Field Pipeline: SHARPs - Space-Weather HMI Active Region Patches. *Sol. Phys.* **289**, 3549. [DOI](#). [ADS](#).

Chen, A.Q., Wang, J.X., Li, J.W., Feynman, J., Zhang, J.: 2011, Statistical properties of superactive regions during solar cycles 19-23. *Astron. Astrophys.* **534**, A47. [DOI](#). [ADS](#).

Chowdhury, P., Kilcik, A., Saha, A., Rozelot, J.-P., Obrikko, V., Erdélyi, R.: 2024, Temporal and Periodic Analysis of Penumbra-Umbra Ratio for the Last Four Solar Cycles. *Sol. Phys.* **299**, 19. [DOI](#). [ADS](#).

Frisch, U.: 1995, *Turbulence. The legacy of A.N. Kolmogorov.* [DOI](#). [ADS](#).

Gao, P.X.: 2019, Association of X-class flares with sunspot groups of various classes in Cycles 22 and 23. *Mon. Not. R. Astron. Soc.* **484**, 5692. [DOI](#). [ADS](#).

Gao, P.X., Xu, J.C.: 2024, Relationship between the Tilt Angles of Sunspot Groups and the Properties of the Next Solar Cycle. *Astrophys. J.* **974**, 268. [DOI](#). [ADS](#).

Gnevyshev, M.N.: 1963, The Corona and the 11-Year Cycle of Solar Activity. *Soviet Astron.* **7**, 311. [ADS](#).

Grotorian, W., Künzel, H.: 1950, Über den Induktionsfluß durch die Sonnenflecken. Mit 12 Textabbildungen. *Zeit. Astrophys.* **28**, 28. [ADS](#).

Guo, J., Lin, J., Deng, Y.: 2014, The dependence of flares on the magnetic classification of the source regions in solar cycles 22-23. *Mon. Not. R. Astron. Soc.* **441**, 2208. [DOI](#). [ADS](#).

Hale, G.E., Ellerman, F., Nicholson, S.B., Joy, A.H.: 1919, The Magnetic Polarity of Sun-Spots. *Astrophys. J.* **49**, 153. [DOI](#). [ADS](#).

Hathaway, D.H.: 2015, The Solar Cycle. *Liv. Rev. Solar Phys.* **12**, 4. [DOI](#). [ADS](#).

Jaeggli, S.A., Norton, A.A.: 2016, The Magnetic Classification of Solar Active Regions 1992-2015. *Astrophys. J. Lett.* **820**, L11. [DOI](#). [ADS](#).

Javaraiah, J.: 2012, The G-O Rule and Waldmeier Effect in the Variations of the Numbers of Large and Small Sunspot Groups. *Sol. Phys.* **281**, 827. [DOI](#). [ADS](#).

Javaraiah, J.: 2013, Long-term temporal variations in the areas of sunspot groups. *Advances in Space Research* **52**, 963. [DOI](#). [ADS](#).

Javaraiah, J.: 2016, North-south asymmetry in small and large sunspot group activity and violation of even-odd solar cycle rule. *Astrophys. Space Sci.* **361**, 208. [DOI](#). [ADS](#).

Jiang, J., Cameron, R.H., Schüssler, M.: 2014, Effects of the Scatter in Sunspot Group Tilt Angles on the Large-scale Magnetic Field at the Solar Surface. *Astrophys. J.* **791**, 5. [DOI](#). [ADS](#).

Jiang, J., Cameron, R.H., Schmitt, D., Schüssler, M.: 2011, The solar magnetic field since 1700. I. Characteristics of sunspot group emergence and reconstruction of the butterfly diagram. *Astron. Astrophys.* **528**, A82. [DOI](#). [ADS](#).

Kashapova, L.K., Zhukova, A.V., Miteva, R., Zhdanov, D.A., Myagkova, I.N., Meshalkina, N.S.: 2021, Analysis of the Properties of SEP Events and Their Solar Sources Taking Into Account of the Magneto-Morphological Classification of Active Regions. *Geomagnetism and Aeronomy* **61**, 1022. [DOI](#). [ADS](#).

Kilcik, A., Yurchyshyn, V.B., Abramenko, V., Goode, P.R., Ozguc, A., Rozelot, J.P., Cao, W.: 2011, Time Distributions of Large and Small Sunspot Groups Over Four Solar Cycles. *Astrophys. J.* **731**, 30. [DOI](#). [ADS](#).

Kitchatinov, L.L.: 2014, The solar dynamo: Inferences from observations and modeling. *Geomagnetism and Aeronomy* **54**, 867. [DOI](#). [ADS](#).

Knizhnik, K.J., Linton, M.G., DeVore, C.R.: 2018, The Role of Twist in Kinked Flux Rope Emergence and Delta-spot Formation. *Astrophys. J.* **864**, 89. [DOI](#). [ADS](#).

Krause, F., Rädler, K.-H.: 1980, *Mean-field magnetohydrodynamics and dynamo theory.* [ADS](#).

Kutsenko, A.S.: 2021, The rotation rate of solar active and ephemeral regions - I. Dependence on morphology and peak magnetic flux. *Mon. Not. R. Astron. Soc.* **500**, 5159. [DOI](#). [ADS](#).

Kutsenko, A.S., Abramenko, V.I., Plotnikov, A.A.: 2024, A Statistical Study of Magnetic Flux Emergence in Solar Active Regions Prior to Strongest Flares. *Research in Astronomy and Astrophysics* **24**, 045014. [DOI](#). [ADS](#).

Leighton, R.B.: 1964, Transport of Magnetic Fields on the Sun. *Astrophys. J.* **140**, 1547. [DOI](#). [ADS](#).

Mandal, S., Banerjee, D.: 2016, Sunspot Sizes and the Solar Cycle: Analysis Using Kodaikanal White-light Digitized Data. *Astrophys. J. Lett.* **830**, L33. [DOI](#). [ADS](#).

Mandal, S., Hegde, M., Samanta, T., Hazra, G., Banerjee, D., Ravindra, B.: 2017, Kodaikanal digitized white-light data archive (1921-2011): Analysis of various solar cycle features. *Astron. Astrophys.* **601**, A106. [DOI](#). [ADS](#).

Mandal, S., Krivova, N.A., Cameron, R., Solanki, S.K.: 2021, On the size distribution of spots within sunspot groups. *Astron. Astrophys.* **652**, A9. [DOI](#). [ADS](#).

Maunder, E.W.: 1903, Spoerer's law of zones. *The Observatory* **26**, 329. [ADS](#).

Maunder, E.W.: 1904, Note on the Distribution of Sun-spots in Heliographic Latitude, 1874-1902. *Mon. Not. R. Astron. Soc.* **64**, 747. [DOI](#). [ADS](#).

McClintock, B.H., Norton, A.A., Li, J.: 2014, Re-examining Sunspot Tilt Angle to Include Anti-Halo Statistics. *Astrophys. J.* **797**, 130. [DOI](#). [ADS](#).

McIntosh, P.S.: 1990, The Classification of Sunspot Groups. *Sol. Phys.* **125**, 251. [DOI](#). [ADS](#).

Moffatt, H.K.: 1978, *Magnetic Field Generation in Electrically Conducting Fluids*, Cambridge Univ. Press, Cambridge, UK. [ADS](#).

Mordvinov, A.V., Kitchatinov, L.L.: 2019, Evolution of the Sun's Polar Fields and the Poleward Transport of Remnant Magnetic Flux. *Sol. Phys.* **294**, 21. [DOI](#). [ADS](#).

Mordvinov, A.V., Karak, B.B., Banerjee, D., Golubeva, E.M., Khlystova, A.I., Zhukova, A.V., Kumar, P.: 2022, Evolution of the Sun's activity and the poleward transport of remnant magnetic flux in Cycles 21-24. *Mon. Not. R. Astron. Soc.* **510**, 1331. [DOI](#). [ADS](#).

Muñoz-Jaramillo, A., Senkpiel, R.R., Windmueler, J.C., Amouzou, E.C., Longcope, D.W., Tlatov, A.G., Nagovitsyn, Y.A., Pevtsov, A.A., Chapman, G.A., Cookson, A.M., Yeates, A.R., Watson, F.T., Balmaceda, L.A., DeLuca, E.E., Martens, P.C.H.: 2015, Small-scale and Global Dynamos and the Area and Flux Distributions of Active Regions, Sunspot Groups, and Sunspots: A Multi-database Study. *Astrophys. J.* **800**, 48. [DOI](#). [ADS](#).

Nagovitsyn, Y.A.: 2024, The Ratio of the Areas of a Sunspot and Its Umbra: Two Populations of Sunspot Groups. *Astronomy Letters* **50**, 329. [DOI](#). [ADS](#).

Nagovitsyn, Y.A., Osipova, A.A.: 2018, The Gnevyshev-Ohl Rule and Two Sunspot Group Populations. *Geomagnetism and Aeronomy* **58**, 1103. [DOI](#). [ADS](#).

Nagovitsyn, Y.A., Ivanov, V.G., Osipova, A.A.: 2019, Features of the Gnevyshev-Waldmeier Rule for Various Lifetimes and Areas of Sunspot Groups. *Astronomy Letters* **45**, 695. [DOI](#). [ADS](#).

Nagovitsyn, Y.A., Osipova, A.A., Nagovitsyna, E.Y.: 2021, "Generative" Indices of Sunspot Solar Activity: 145-Year Composite Series. *Sol. Phys.* **296**, 32. [DOI](#). [ADS](#).

Nagovitsyn, Y.A., Pevtsov, A.A., Osipova, A.A.: 2017, Long-term variations in sunspot magnetic field-area relation. *Astronomische Nachrichten* **338**, 26. [DOI](#). [ADS](#).

Nagovitsyn, Y., Pevtsov, A., Osipova, A.: 2023, Two Populations of Sunspot Groups and Their Meridional Motions. *Sol. Phys.* **298**, 108. [DOI](#). [ADS](#).

Nagovitsyn, Y.A., Pevtsov, A.A., Osipova, A.A., Tlatov, A.G., Miletskii, E.V., Nagovitsyna, E.Y.: 2016, Two populations of sunspots and secular variations of their characteristics. *Astron. Lett.* **42**, 703. [DOI](#). [ADS](#).

Nagovitsyn, Y.A., Pevtsov, A.A., Osipova, A.A., Ivanov, V.G.: 2018, Some Features of the Two Sunspot Group Populations' Properties. *Geomagnetism and Aeronomy* **58**, 1170. [DOI](#). [ADS](#).

Nagy, M., Lemerle, A., Labonville, F., Petrovay, K., Charbonneau, P.: 2017, The Effect of "Rogue" Active Regions on the Solar Cycle. *Solar Phys.* **292**, 167. [DOI](#). [ADS](#).

Norton, A.A., Levens, P.J., Knizhnik, K.J., Linton, M.G., Liu, Y.: 2022, Characterizing the Umbral Magnetic Knots of  $\delta$ -Sunspots. *Astrophys. J.* **938**, 117. [DOI](#). [ADS](#).

Obrikko, V.N., Badalyan, O.G.: 2014, Cyclic and secular variations sunspot groups with various scales. *Astron. Rep.* **58**, 936. [DOI](#). [ADS](#).

Parker, E.N.: 1955, Hydromagnetic Dynamo Models. *Astrophys. J.* **122**, 293. [DOI](#). [ADS](#).

Scherrer, P.H., Bogart, R.S., Bush, R.I., Hoeksema, J.T., Kosovichev, A.G., Schou, J., Rosenberg, W., Springer, L., Tarbell, T.D., Title, A., Wolfson, C.J., Zayer, I., MDI Engineering Team: 1995, The Solar Oscillations Investigation - Michelson Doppler Imager. *Sol. Phys.* **162**, 129. [DOI](#). [ADS](#).

---

Scherrer, P.H., Schou, J., Bush, R.I., Kosovichev, A.G., Bogart, R.S., Hoeksema, J.T., Liu, Y., Duvall, T.L., Zhao, J., Title, A.M., Schrijver, C.J., Tarbell, T.D., Tomczyk, S.: 2012, The Helioseismic and Magnetic Imager (HMI) Investigation for the Solar Dynamics Observatory (SDO). *Sol. Phys.* **275**, 207. [DOI](#). [ADS](#).

Sokoloff, D., Khlystova, A., Abramenko, V.: 2015, Solar small-scale dynamo and polarity of sunspot groups. *Mon. Not. R. Astron. Soc.* **451**, 1522. [DOI](#). [ADS](#).

Suleimanova, R.A., Abramenko, V.I.: 2024, Manifestations of the Turbulent Component of the Global Solar Dynamo in an Activity Minimum. *Geomagnetism and Aeronomy* **63**, 1136. [DOI](#). [ADS](#).

Suleymanova, R.A., Miroshnichenko, L.I., Abramenko, V.I.: 2024, Magnetic Configuration of Active Regions Associated with GLE Events. *Sol. Phys.* **299**, 7. [DOI](#). [ADS](#).

Toriumi, S., Wang, H.: 2019, Flare-productive active regions. *Liv. Rev. Solar Phys.* **16**, 3. [DOI](#). [ADS](#).

Usoskin, I.G., Kovaltsov, G.A., Chatzistergos, T.: 2016, Dependence of the Sunspot-Group Size on the Level of Solar Activity and its Influence on the Calibration of Solar Observers. *Sol. Phys.* **291**, 3793. [DOI](#). [ADS](#).

van Driel-Gesztelyi, L., Green, L.M.: 2015, Evolution of Active Regions. *Liv. Rev. Solar Phys.* **12**, 1. [DOI](#). [ADS](#).

Wang, Y.-M., Sheeley, J. N. R.: 1989, Average Properties of Bipolar Magnetic Regions during Sunspot CYCLE-21. *Sol. Phys.* **124**, 81. [DOI](#). [ADS](#).

Zhang, J., Wang, Y., Liu, Y.: 2010, Statistical Properties of Solar Active Regions Obtained from an Automatic Detection System and the Computational Biases. *Astrophys. J.* **723**, 1006. [DOI](#). [ADS](#).

Zhukova, A.: 2018, A catalog of active regions of the 24th solar cycle. *Izv. Krym. Astrofiz. Obs.* **114**, 74. [DOI](#). [URL](#).

Zhukova, A.: 2024, Hemispheric analysis of the magnetic flux in regular and irregular solar active regions. *Mon. Not. R. Astron. Soc.* **532**, 2032. [DOI](#). [ADS](#).

Zhukova, A.V., Abramenko, V.I., Suleymanova, R.A.: 2024, Comparative Features of the North-South Asymmetry of Solar Activity According to Data on the Number and Magnetic Fluxes of Active Regions of Different Magnetic Morphology in the 23rd and 24th Cycles. *Geomagnetism and Aeronomy* **64**, 1004. [DOI](#). [ADS](#).

Zhukova, A., Khlystova, A., Abramenko, V., Sokoloff, D.: 2020, A Catalog of Bipolar Active Regions Violating the Hale Polarity Law, 1989 - 2018. *Sol. Phys.* **295**, 165. [DOI](#). [ADS](#).

Zhukova, A., Khlystova, A., Abramenko, V., Sokoloff, D.: 2022, Synthetic solar cycle for active regions violating the Hale's polarity law. *Mon. Not. R. Astron. Soc.* **512**, 1365. [DOI](#). [ADS](#).

Zhukova, A., Sokoloff, D., Abramenko, V., Khlystova, A.: 2023, The north-south asymmetry of active regions of different magneto-morphological types in solar cycles 23 and 24. *Advances in Space Research* **71**, 1984. [DOI](#). [ADS](#).